

1 ***Ehrlichia ruminantium* uses its transmembrane protein Ape to adhere to**
2 **host bovine aortic endothelial cells**

3
4 Valérie Pinarello^{1,2#}, Elena Bencurova³, Isabel Marcelino⁴, Olivier Gros⁵, Carinne Puech²,
5 Mangesh Bhide^{3,6}, Nathalie Vachery² and Damien F. Meyer^{1,2*}.

6
7 ¹CIRAD, UMR ASTRE, F-97170 Petit-Bourg, Guadeloupe, France

8 ²ASTRE, CIRAD, INRA, Univ Montpellier, Montpellier, France

9 ³ Laboratory of biomedical microbiology and immunology, University of veterinary medicine
10 and pharmacy in Kosice, Komenskeho 73, Kosice, Slovakia

11 ⁴ Institut Pasteur de la Guadeloupe, 97183 Les Abymes Cedex, Guadeloupe, France

12 ⁵ Institut de Systématique, Évolution, Biodiversité (ISYEB), Muséum national d'Histoire
13 naturelle, CNRS, Sorbonne Université, EPHE, Université des Antilles
14 Campus de Fouillole, 97110 Pointe-à-Pitre, France

15 ⁶ Institute of neuroimmunology, Slovak academy of sciences, Bratislava, Dubravska cesta
16 9, Slovakia

17

18 # present address: CIRAD, UMR ASTRE, Harare, Zimbabwe

19 *Email: damien.meyer@cirad.fr

20

21 **Abstract**

22 *Ehrlichia ruminantium* is an obligate intracellular bacterium, transmitted by ticks of the genus
23 *Amblyomma* and responsible for heartwater, a disease of domestic and wild ruminants. High
24 genetic diversity of *E. ruminantium* strains hampers the development of an effective vaccine
25 against all strains present in the field. In order to develop strategies for the control of
26 heartwater through both vaccine and alternative therapeutic approaches, it is important to
27 first gain a better understanding of the early interaction of *E. ruminantium* and its host cell.
28 Particularly, the mechanisms associated with bacterial adhesion remain to [be elucidated](#).
29 Herein, we studied the role of *E. ruminantium* membrane protein ERGA_CDS_01230
30 (UniProt Q5FFA9), a probable iron transporter, in the adhesion process to host bovine aortic
31 endothelial cells (BAEC). The recombinant version of the protein ERGA_CDS_01230,
32 successfully produced in the *Leishmania tarentolae* system, is O-glycosylated. Following *in*
33 *vitro* culture of *E. ruminantium* in BAEC, the expression of CDS ERGA_CDS_01230 peaks
34 at the extracellular infectious elementary body stages. This result suggest the likely
35 involvement of ERGA_CDS_01230, named hereafter Ape for Adhesion protein of *Ehrlichia*,
36 in the early interaction of *E. ruminantium* with its host cells. We showed using flow cytometry
37 and scanning electron microscopy that beads coated with recombinant ERGA_CDS_01230
38 (rApe) adheres to BAEC. In addition, we also observed that rApe interacts with proteins of
39 the cell lysate, membrane and organelle fractions. Additionally, enzymatic treatment
40 degrading dermatan and chondroitin sulfates on the surface of BAEC is associated with a
41 50% reduction in the number of bacteria in the host cell after a development cycle, indicating
42 that glycosaminoglycans seem to play a role in the adhesion of *E. ruminantium* to the host
43 cell. Finally, Ape induces a humoral response in vaccinated animals. Globally, our work
44 identifying the role of Ape in *E. ruminantium* adhesion to host cells makes it a gold vaccine
45 candidate and represents a first step toward the understanding of the mechanisms of cell
46 invasion by *E. ruminantium*.

47

48 **Introduction**

49 *Ehrlichia ruminantium* is an obligate intracellular Gram-negative bacterium responsible for
50 the fatal and neglected heartwater disease of domestic and wild ruminants (Allsopp, 2010).

51 This bacterium belongs to the Anaplasmataceae family in the order Rickettsiales that
52 includes many pathogens and symbionts of veterinary and public health importance
53 (Moumene and Meyer, 2015). *E. ruminantium* is transmitted by ticks of the genus

54 *Amblyomma* in the tropical and sub-Saharan areas, as well as in the Caribbean islands. It

55 constitutes a major threat for the American livestock industries since a suitable tick vector is
56 already present in the American mainland and potential introduction of infected *A.*

57 *variegatum* through migratory birds or uncontrolled movement of animals from Caribbean
58 could occur (Deem, 1998). Kasari et al., 2010). The disease is also a major obstacle to the

59 introduction of animals from heartwater-free to heartwater-infected areas into sub-Saharan
60 Africa and thus restrains the breeding to upgrade local stocks (Allsopp, 2010). The small

61 genome of *E. ruminantium* (1.5 Mb) shows an unique process of contraction/expansion in
62 non-coding regions and targeted at tandem repeats (Frutos et al., 2006). This genome

63 plasticity, associated with a high genetic diversity, suggests a capacity of adaptation upon
64 exposure to a novel environment and could also explain the low field efficacy of available

65 vaccines (Cangi et al., 2016).

66 After adhesion and entry of infectious elementary bodies into host cells, *E. ruminantium*
67 replicates by binary fission of reticulated bodies into an intracellular vacuole bounded by a

68 lipid bilayer membrane derived from the eukaryotic host endothelial cell membrane (Dumler
69 et al., 2001). *Ehrlichia* spp. have evolved sophisticated mechanisms to invade and multiply

70 in host tissues by hijacking/subverting host cell processes ranging from host signaling,
71 modulation of vesicular traffic, protection from oxidative burst, acquisition of nutrients, and

72 control of innate immune activation (Moumene and Meyer, 2015). Notably, *E. chaffeensis*
73 secretes the type IV effector Etf-1 to induce autophagy and capture nutrients, whereas it

74 uses Etf-2 to delay endosome maturation to avoid phagolysosomal fusion for the benefit of
75 bacterial replication (Lin et al., 2016; Yan et al., 2018). Moreover, recent work identified that

76 *E. chaffeensis* uses EtpE invasin to enter mammalian cells via the binding to its receptor
77 DNaseX, a glycosylphosphatidylinositol-anchored cell surface receptor (Mohan Kumar et

78 al., 2013). That receptor-triggered entry simultaneously blocks the generation of reactive
79 oxygen species (ROS) by host monocytes and macrophages (Teymournejad et al., 2017).

80 Due to the lack of some key metabolic genes that are required for host-free living and
81 similarly to what is observed in other intracellular bacteria, entry into the eukaryotic host

a mis en forme : Police :Non Italique

a mis en forme : Police :Non Italique

a supprimé: , and

a supprimé: ongoing

a supprimé: but

a supprimé: for

86 cells is crucial for *E. ruminantium* to sustain its life and disseminate (Pizarro-Cerda and
87 Cossart, 2006) ; (Frutos et al., 2007). Computational studies have predicted type IV effectors
88 in *E. ruminantium* (Noroy et al., 2019) which, however, remain to be characterized; the
89 mechanisms of adhesion and entry are still unknown and may be active or passive
90 depending on the pathogen. *E. ruminantium* could either inject a type IV effector across
91 the host cell membrane to trigger actin rearrangement and pathogen phagocytosis such as
92 *Bartonella henselae* (Truttmann et al., 2011). An another option is the use of homologous
93 system of *E. chaffeensis* invasion/receptor pair (Mohan Kumar et al., 2013) or an outer
94 membrane protein of the OmpA family that actively trigger internalization as was observed
95 in *Coxiella burnetii* (Martinez et al., 2014).

96 Bacterial pathogens are capable of exploiting and diverting host components such as
97 proteoglycans for their pathogenesis (Aquino et al., 2018). These assemblies of
98 glycosaminoglycans (GAGs) chains fixed around a protein nucleus (Bartlett and Park, 2010)
99 are expressed constitutively on the cell surface, in intracellular compartments as well as in
100 the extracellular matrix. They are known to act as receptors for pathogens in many cases of
101 infection (Aquino et al., 2018); (Rajas et al., 2017); (Gagoski et al., 2015). Many pathogens
102 – e.g. *Chlamydia trachomatis* with a biphasic life cycle like *E. ruminantium* – use GAGs as
103 an initial anchor site of low affinity; this facilitates interaction with their respective secondary
104 receptor allowing internalization but GAGs are sometimes also used as bridging molecules
105 (Aquino et al., 2010). Thus, whether *E. ruminantium* uses GAGs as a portal of entry or any
106 specific bacterial surface protein is unknown but essential for developing any anti-infective
107 measures.

108 The outer membrane proteome study of *E. ruminantium* Gardel strain revealed that a
109 hypothetical protein, the possible major ferric iron binding protein precursor the putative iron
110 transporter ERGA_CDS_01230, is uniquely expressed in the outer-membrane fraction
111 (Moumene et al., 2015). This protein was also shown to be O-glycosylated only in *E.*
112 *ruminantium* (Marcelino et al. 2019). Moreover, homologous counterparts of this protein in
113 other pathogenic species play a key role in bacterial survival within the host by scavenging
114 iron from mammalian serum iron transport proteins (Brown et al., 2010). Interestingly, we
115 previously showed that iron starvation induces expression of virulence factors such as type
116 IV secretion genes (Moumene et al., 2017).

117 In this study, we show that ERGA_CDS_01230 (UniProt Q5FFA9, named herein Ape for
118 Adhesion protein of *Ehrlichia ruminantium*,) is involved in the binding of *E. ruminantium* to
119 bovine aortic endothelial cells (BAEC). In order to study whether Ape alone can mediate the

a mis en forme : Police :Italique

a supprimé: Computational studies allowed the prediction of type IV effectors for *E. ruminantium*

a supprimé: that remain to be fully characterized but detailed mechanisms of adhesion and entry are still unknown. These processes can be active or passive depending on the pathogen

126 invasion of host cells by adhering to endothelial cells membrane, we used latex beads
127 coated with recombinant Ape. These beads covered with the protein adhered and seemed
128 to enter endothelial cells similarly to what is observed with *E. ruminantium in vitro* (Moumene
129 and Meyer, 2015). Subsequent investigation uncovered that rApe is a glycosylated protein
130 that induces a strong humoral immune response in vaccinated goats making it a possible
131 vaccine candidate.

132

133 **Methods**

134 **Synchronous culture**

135 *E. ruminantium* (strain Gardel) was propagated in Bovine Aortic endothelial cells (BAEC
136 isolated at CIRAD, Guadeloupe, France) in Baby Hamster Kidney (BHK-21) cell medium
137 supplemented with 1% L-glutamine 200mM (Eurobio), 10% heat-inactivated fetal bovine
138 serum (FBS, Thermofisher), 1% penicillin 10000UI/ streptomycin 10000 µg (Eurobio), 1x
139 amphotericin B (Sigma), 5% NaHCO₃ 5.5%, under 5% CO₂ at 37°C modified from
140 (Marcelino et al., 2005). The cell trypsinization (Trypsin-Versen, Eurobio) was carried out
141 with a splitting ratio of ½ when monolayer reached 100% confluence. Synchronous infection
142 of a new BAEC monolayer was obtained using a bacterial suspension previously harvested
143 at 120 hpi by scraping the TC flask (TCF) and passing infected lysed cells through 18G and
144 26G needles before reinfection at a ratio of 1/20 (Marcelino et al., 2005).

145

146 **Quantitative reverse transcription RT-PCR along bacterial cycle**

147 *E. ruminantium*-infected BAE cells were harvested for RNA extraction by trypsinization at
148 24, 48, 72 and 96 hours post infection (hpi), centrifuged 1700 x g, 5 min at 4°C and by cell
149 lysate scrapping at 120 hpi, centrifuged 20000 x g, 15 min at 4°C. All pellets were dissolved
150 in 1 mL TRIZOL (Thermofisher), RNA was extracted following manufacturer's
151 recommendations and eluted in 100 µL H₂O RNase/DNase free. RNA was treated by Turbo
152 DNase (Ambion) according to supplier's instructions and precipitated overnight at -20°C in
153 2.5 volume (v/v) cold absolute ethanol (Normapur), 1/10 volume of 3 M sodium acetate and
154 1 µL glycogen 10 mg/mL (Thermofisher). Pellet obtained by centrifugation 15000 x g, 10
155 min, 4°C was washed with 1 mL 75% ethanol, air dried after centrifugation 9000 x g, 7 min,
156 4°C and dissolved in 20 µL H₂O RNase/ DNase free. Two µg ARN were reverse transcribed
157 using "SuperScript™ VILO™ cDNA Synthesis Kit" (Invitrogen), according to the supplier's
158 specifications.

159 **Pre amplification of *ape* gene**

160 Quantification started by 15 cycles of pre-amplification (same reaction mix and cycling
161 conditions as below). ERGA_CDS_01230 (Ape) was amplified in 25 µL reaction mix
162 containing 250 nM of the forward ERGA_CDS_01230F AATGGAGAATGAGGGGGAAG
163 and reverse ERGA_CDS_01230R ACCCAAACCAAATCCATCA primers, 12.5 µL of
164 Power SYBR® Green PCR Master Mix (ThermoFisher), 12.5 µL H₂O RNase/ DNase free
165 and 20 µL pre-amplified DNA. Reactions were performed in a Quantstudio 5 (ThermoFisher)
166 as follow: 50°C, 2 min for Uracil-N-Glycosylase activation, 95°C, 10 min for Uracil-N-
167 Glycosylase inactivation and polymerase activation; 40 cycles 95°C, 15 sec denaturation
168 and 59°C, 60 sec hybridization and elongation. The specificity of the PCR product was
169 confirmed by the dissociation curves.

a supprimé: A

a mis en forme : Police :Italique

a mis en forme : Police :Gras

170 **Quantification of *E. ruminantium* along the bacterial cycle**

171 *E. ruminantium* quantification for normalization as described by (Pruneau et al., 2012), was
172 performed by DNA extraction according to manufacturer's specifications (QiaAmp DNA
173 minikit, QIAGEN, Courtaboeuf) on 1/10 of the harvested volume, after 20000 x g, 15 min
174 centrifugation and dissolution in 200 µL PBS 1x, followed by a [quantitative polymerase chain
175 reaction \(qPCR\)](#) *So1* targeting the pCS20 region (Cangi et al., 2017).

a mis en forme : Police :Italique

a mis en forme : Police :Gras

176 **Normalization of *ape* gene expression**

177 Normalization by *E. ruminantium* quantification was calculated: $R_{x\ hpi} = [cDNA\ copy\ number$
178 $(ERGA_CDS_01230)] / [E.\ ruminantium\ pCS20\ DNA\ copy\ number]$, allowing fold change (FC)
179 determination, compared to expression at 96 hpi (corresponding to the stationary phase of
180 the bacterial growth): $FC = R_{x\ hpi} / R_{96\ hpi}$. Results were represented in log₂, according to
181 Pruneau et al. (2012) and confirmed by 2 others [biological replicates](#) (data not shown).

a supprimé: qPCR

a supprimé: A

a mis en forme : Police :Gras

a mis en forme : Police :Italique

a mis en forme : Police :Gras, Italique

a mis en forme : Police :Gras

a supprimé: (pCS20)

a supprimé: kinetics

183 **Recombinant protein production**

184 pLEXY_I-blecherry3 plasmid (Bioscience, 2011) and 400 ng of amplified
185 CDS_ERGA_01230 were digested 10 min at 37°C by BamHI and Sall (Thermo Scientific,
186 USA) and column purified (Macherey Nagel, Germany). The digested product was ligated
187 in pLEXY_I-blecherry3 plasmid using T4 DNA Ligase (Thermo Scientific) for 1 h at 22°C.
188 pLEXY_I-blecherry3 plasmid was modified with the addition of a sequence coding GFP at
189 C-terminus of the insert and 6X His tags at N-terminus of insert. It is to note that, GFP and
190 the coding sequence of CDS_ERGA_01230 were linked with the sequence encoding
191 cleavage site for Xa factor. Ligated plasmid was column purified and 50 ng of the ligation
192 mix was electro-transferred to competent bacteria *E. coli* XL10 (Miller and Nickoloff, 1995).

198 100 µL of transformed culture were spread on LB medium Petri dish supplemented with
199 carbenicillin (50µg/ml). To confirm the presence of the plasmid and the insert, a PCR was
200 performed on a colony using vector specific primers (Forward,
201 CGCATCACCATCACCATCAGC; Reverse, ACCAAAATTGGGACAACACCAGTG). PCR
202 product was then sequenced. Transformed E. coli clone was grown 16 h at 37°C under 200
203 rpm stirring until optical density (OD) reached 3. The plasmid was isolated
204 using "GenElute™ Plasmid Midiprep" kit (Sigma Aldrich) and digested with *SmaI* (Thermo
205 Scientific)

206 *Leishmania tarentolae* preculture was grown in 10 mL LEXSY BHI medium with TC flask at
207 26°C. 3 days after, preculture was diluted 10 fold in 10 mL LEXSY BHI medium and
208 incubated overnight at 26°C (flat position). Next day, *Leishmania tarentolae* were
209 centrifuged 5 min (2000 x g) and half of the medium was removed. Cells were resuspended
210 in remaining medium to get 10⁸ cells/ mL and incubated 10 min on ice. 350 µL cells were
211 electroporated at 450 V, 450 µF, 5 - 6 msec impulses with 5 µg linearized plasmid (smal
212 digested). Cells were immediately incubated for 10 min on ice, transfer to 10 mL LEXSY BHI
213 medium (Bioscience) and incubated overnight. 10 µL bleomycin (100 mg/mL, (Bioscience)
214 was then added to nonclonal selection for 3 more days. 5 mL of culture supernatant was
215 centrifuged for 3 min at 1000 x g. Pellet was resuspended in 10 mL LEXSY BHI medium
216 containing bleomycin and incubated at 26°C for 5 days. After nonclonal selection,
217 expression of protein was induced in 45 mL BHI medium supplemented with bleomycin and
218 tetracyclin 10 mg/mL (Bioscience). 5 ml of culture from nonclonal selection was added
219 incubated for 72 h at 26°C with shaking at 100 rpm. Supernatant was harvested and
220 concentrated in dialyses bag (3.5 kDa membrane, Serva) in a polyethylene glycol solution
221 20000 overnight at 4°C. Proteins were concentrated and purified by Sephadex gel filtration.

222 Mass spectrometry analysis

223 Protein size was verified by MALDI-TOF (Microflex, Bruker). The presence of GFP tag and
224 associated fluorescence was checked respectively by immunoblotting and aggregation on
225 Probond beads followed by fluorescence microscopy. Mass spectrometry allowed to check
226 rApe size and Orbitrap allowed to confirm identity of the protein.

227

228 **3D Structure and localization prediction**

229 Protein structure prediction was accomplished using I-TASSER-MTD (Xiaogen Zhou,
230 2022) and view was generated by MacPyMol (DeLano, 2009). The subcellular localization
231 was predicted by "CELLO 2.5: subCELLular LOcalization predictor" (Yu et al., 2006), from

a mis en forme : Police :(Par défaut) Arial, Gras, Couleur de police : Automatique, Anglais (E.U.)

a mis en forme : Police :Gras

a supprimé: MALDI

a supprimé: e.

a supprimé: (Yang and Zhang, 2015;Xiaogen Zhou, 2022) ...

236 the protein sequence, accession number CAI27575.1. Ape structural homology was
237 determined using "Swiss model, Expasy" (Waterhouse et al., 2018).

238

239 **Western Blot for O-GlcNAc Glycoprotein detection**

240 rApe was migrated on an acrylamide gel "SDS page" (NuPAGE bis-tris, Novex) for 2 h 30
241 min at 100V and 400mA in MOPS buffer (Novex), according to the supplier's instructions
242 (Nu PAGE Technical Guide). Approximately 10 µg protein [and BSA for the negative control](#)
243 were denatured at 70°C for 10 min with LDS buffer and reducing agent (Novex) and migrated
244 with a [3.1 to 198 kDa](#) molecular weight marker (SeeBlue plus 2, Invitrogen). A gel-sized PVDF
245 membrane (Amersham, Hybond-P) was soaked for 30 sec in methanol (Normapur) and
246 incubated in transfer buffer (20x, NuPAGE) for at least 15 min with the same size filter
247 papers (Whatman) and 4 sponges. The transfer assembly was performed according to the
248 NuPAGE technical guide and the transfer was run 1 h 15 min at 30 V, 170 mA. The
249 membrane was then immersed in a solution of Culvert Red (AMRESCO) ~1 min and rinsed
250 with water prior to picture. The protocol for western blot detection was modified from
251 (Marcelino et al., 2019). The membrane was blocked for 3 h at room temperature (RT) with
252 stirring in PBS (pH 7.4), 0.05% Tween20 (PBS-T) and 5% milk. Then, membrane was
253 incubated overnight with anti-O-GlcNAc antibody (Santa Cruz), [monoclonal IgM](#), diluted 200
254 fold in blocking solution. After three washes with PBS-T, membrane was incubated with anti-
255 mouse antibody (IgM-HRP, Molecular probes) diluted 1000 fold in PBS-T for one hour. The
256 membrane was washed 3 times 10 min with PBS-T before the addition of the TMB substrate
257 (Pierce) and gel reader picture once the color was developed.

258

259 **Glycosaminoglycans degradation assays**

260 10, 5, 1 and 0.3 µg/ mL heparan sulfate (Jonquieres et al., 2001; Kobayashi et al., 2010) and
261 9 µg/ mL rApe (positive control) were adsorbed in 50 µL of carbonate/bicarbonate buffer pH
262 9.6 (Martinez et al., 1993), distributed in Nunc Maxisorp wells, 1 h at 37°C with gentle stirring
263 then overnight at 4°C. The next day, 3 washes were carried out with 200 µL of PBS-T per
264 well. Blocking was done 1 h at 37°C under agitation with 100 µL of blocking buffer PBS
265 tween 20 0.05% milk 3%, followed by 3 washes with 200 µL of PBS-T per well. 50 µL/ well
266 of rApe at 14.3 µg/mL diluted in PBS tween 20 0.05% milk 3% was incubated 1 h at 37°C
267 with stirring. Three washes of 200 µL PBS-T per well were performed, followed by addition
268 of 50 µL anti-GFP antibody diluted to 4,000 in PBS-T with milk 3% and incubation 1 h at
269 37°C with stirring. Washings were repeated as above. Addition of 200 µL TMB substrate

a supprimé: -

271 allowed revelation within 30 min at 37°C before to stop the reaction with 100 µL of H2SO4
272 2N. The reading was done at 450 nm (Multiskan, Thermofisher). 2 cm² wells were inoculated
273 with ~1.1x10⁴ BAEC in 500 µL BHK21 medium. When confluence was reached, several
274 concentrations of [chondroitinase \(Sigma Aldrich\)](#) were tested as follows: 0.2U, 0.4U and
275 0.9U/ mL [chondroitinase](#) was incubated 2 h before infection with the BAEC in 1X PBS and
276 bovine fetal serum (SBF)-free BHK21 medium (Sava et al., 2009;Rajas et al., 2017). The
277 medium was renewed with standard BKH21 prior infection at a ratio 1/20 and 2 h after
278 infection. At lysis stage, all the wells were scraped, centrifuged for 15 min at 20,000 x g.
279 DNA was extracted using the QiaAmp DNA minikit (Qiagen) and quantified using qPCR™
280 Sol1, targeting the pCS20 region (Cangi et al., 2017). The results were treated using the
281 $\Delta\Delta C_t$ method and represented in $2^{-\Delta\Delta C_t}$.

282

283 **Flow cytometry for attachment quantification**

284 We used the cytometer to quantify the fluorescence-labelled cells following incubation with
285 rApe. Six-well Nunc plates (9.6 cm²/ well) with confluent BAEC were incubated for 2 h at
286 37°C, 5% CO₂ with rApe concentrations ranging from 6.4 to 102.4 µg/ mL following the
287 principle described in (Lundberg et al., 2003). The negative control consisted of confluent
288 BAE cells. After incubation with recombinant protein, each well was rinsed twice with 1 mL
289 of 1X PBS and 1.5 mL of 1X PBS was used to scrape the well. After centrifugation during
290 10 min at 200 x g, at 4°C cells were resuspended in Isoflow (Beckman) for further reading
291 the percentage of fluorescent labelled cells on the cytometer (FC500, Beckman Coulter).

292

293 **Far Western Blot**

294 The BHK21 culture medium of a 175 cm² TCF was removed, the TCF was washed with 5mL
295 of PBS 1x containing anti-protease (Roche). ~10mL of cold PBS 1x was added to gently
296 scrap the cell mat. Centrifugation 10 min at 200 x g and 4°C was performed to remove the
297 supernatant. Lysis of the pellet was performed by addition of 3 mL native lysis buffer (150
298 mM NaCl, 50 mM Tris-HCl, pH 7.4, NP-40 1%, anti-proteases 1%), followed by 4
299 "freeze/thaw" cycles by first immersing the lysate 2 min in an ethanol/ ice bath, then 2 min
300 in a 37°C water bath. The lysate was vortexed between each bath. The cells were broken
301 by passing the lysate 4 times through an 18G needle with a syringe. The cell debris were
302 pelleted at 10000 x g for 30 min prior to supernatant transfer into a new tube.

303 Four different fractions (F1, cytosol components; F2, membrane and organelle components;
304 F3, nucleus components; F4, the cytoskeleton) were extracted using the "ProteoExtract

a supprimé: chondroitinase

a supprimé: chondroitinase

307 Subcellular Proteome Extraction kit" (Calbiochem/ MERCK) according to the supplier's
308 instructions. Each fraction was placed in acetone (at least 5x the volume of the extracted
309 fraction) for overnight precipitation at -20°C. The day after, each pellet was re-suspended in
310 500µL of native lysis buffer after 20 min centrifugation at 15000 x g and 4°C.
311 18 µL of each cell fraction and 35 µL of lysate were migrated onto acrylamide gel, with
312 addition of LDS, under the same conditions as for the glycosylation tests (but without
313 addition of reducing agent or heating), as well as for the transfer onto PVDF membrane.
314 The membrane was stored in TTBS 1x (10mM TRIS, 150mM NaCl, 0.05% Tween 20, pH
315 8,3), then blocked for 1 h at RT under gentle agitation in 2% Bovine Serum Albumine (BSA)
316 in TTBS and finally rinsed 3 times for 5 min with TTBS. The membrane was incubated
317 overnight at 4°C under slow rotation with 0.5 mg rApe in 1% BSA in TTBS. The negative
318 control (without recombinant protein) was incubated in the same conditions. The next day,
319 the membrane was washed 3x for 5 min with TTBS and incubated 1 h at RT under agitation
320 with anti-GFP-HRP (Thermofisher) diluted 2,500 fold in 1% BSA in TTBS. The membrane
321 was washed again 3 x for 5 min with TTBS. The binding of anti- GFP-HRP was revealed by
322 the addition of 4.5 mL peroxide substrate (Pierce Thermofisher) + 0.5mL chromogen DAB
323 (Thermofisher) and incubation 10 min at RT. Picture was taken by colorimetry reading.

324

325 **Scanning electronic microscopy for binding assays**

326 Two kinds of fluorescent latex beads (with a sulfate group) were adsorbed with rApe through
327 electrostatic interactions based on (Martinez et al., 2014). A total of 10^{10} beads (0.1 µm in
328 diameter) and 7×10^9 beads (0.5 µm in diameter) were adsorbed with 100 µg/mL rApe in 1
329 mL of 25 mM MES, pH 6.1 (Sigma Aldrich) during 4h at RT under slow rotation. Then, three
330 washes were performed using the same buffer before to be resuspended in 1 mL of 1% BSA
331 MES. 24-well plates containing 13 mm diameter lamellae (VWR) were inoculated with
332 BAEC. A deposit of 0.1 or 0.5 µm-diameter beads (1.82×10^8 per well) was made in BHK21
333 medium. The negative control consisted of recombinant protein-free beads incubated with
334 BAEC. The plate was centrifuged 5 min at 200 x g at RT before incubation 30-120 min at
335 37°C under 5% CO₂ atmosphere. Three washes with PBS 1X removed the excess of
336 unbound beads before overnight fixation with 2% paraformaldehyde. Lamellae were then
337 removed from each well and dehydrated in series of acetone solutions of increasing
338 concentration, dried to critical point in CO₂ and sputter-coated with gold before observation
339 with a FEI Quanta 250 electron microscope at 20 kV.

340

341 ELISA-based binding assays

342 The antibody response to Ape during vaccination of goats was tested by ELISA. Sera for
343 vaccinated goats obtained from previous studies (Marcelino et al. 2015 a, b) were incubated
344 in wells coated with rApe, followed by incubation with anti-goat [IqG](#) antibody coupled to
345 HRP.

346 The adsorption of [4 µg/ mL](#) rApe diluted in 100 µL of carbonate bicarbonate buffer pH 9.6
347 was performed in a Nunc plate (Maxisorp). One hour incubation was carried out at 37°C with
348 stirring at 150 rpm then overnight at 4°C. The plate was washed with 300 µL/ well of wash
349 buffer (PBS 1x pH 7.2, Tween 20 0.1%). Blocking was carried out at 37°C with stirring in
350 300 µL blocking buffer (PBS1x, tween 20 0.1%, casein 2%) for 1 h. Washings were repeated
351 as described in the previous step. 100 µL of each goat serum diluted 100-fold in blocking
352 buffer was incubated 1 h at 37°C with agitation (Perez et al., 1998); 2 blank wells were
353 incubated with 100 µL blocking buffer. Five washes with Wash Buffer preceded the deposit
354 of 100 µL of anti-goat [IqG](#) antibody (Rockland) diluted 20,000-fold in blocking buffer and 1
355 h incubation at 37°C with agitation. Five washes were performed. The revelation was
356 performed by addition of 100 µL of TMB (Neogen) and stopping of the reaction after 5 min
357 development by the addition of 50 µL of 0.5 M H₂SO₄. Antibody response was detected by
358 ELISA titers and optical density (OD) was read with a spectrophotometer at 450nm. The OD
359 of the wells without serum were valid when < 0.1 ; OD of negative samples were valid when
360 < 0.2.

361

362 Results

363

364 ERGA_CDS_01230 (*ape*) is highly expressed at infectious elementary body stages of 365 *E. ruminantium* development inside mammalian cells.

366 In order to measure the expression of the *ape* gene, normalization was carried out in relation
367 to the number of bacteria present at each stage of development since no reference gene
368 with a sufficiently stable expression is available for *E. ruminantium*. The development cycle
369 of *E. ruminantium* is synchronized when the lysis occurs 5 days after BAEC infection.
370 Quantification of the number of bacteria present in the BAEC every 24 hpi by qPCR Sol1
371 showed a sigmoidal curve represented in log₁₀ (Figure 1A). The bacterium had a slow
372 growth phase between 24 and 48 hpi then an exponential development with a slowing down
373 of the growth, a stationary phase after 96 hpi and a maximum of copies reached at 120 h
374 (release of elementary bodies). The number of transcripts was determined by qPCR and a

a supprimé: four

a supprimé:

377 ratio calculated at each time as follow: (*E. ruminantium* cDNA number) / (*E. ruminantium* pCS20
378 DNA copy number). The fold change (FC) was determined in relation to bacterial expression at 96
379 hpi (stationary phase) and represented graphically in Figure 1B. The expression of *ape*
380 gene peaks at the elementary body infectious stages of *E. ruminantium* life cycle which
381 correspond to 120 hpi (host cell lysis) and 24 hpi (lag phase). These data indicate that *ape*
382 is expressed when the bacterium is released and ready to infect new cells.

a mis en forme : Indice

384 **Ape protein presents a C-clamp structure and is predicted to be an outer-membrane** 385 **protein**

386 The 3D structure proposed by I-TASSER-[MTD](#) software (Figure 2A) showed that Ape
387 harbours a succession of helices α linked by loops distributed around a β sheet and showed
388 a "c-clamp" three-dimensional structure. By homology with other known I^{ry}, II^{ry} or III^{ry}
389 structures, "Swiss model" showed a strong analogy of Ape with a "C-clamp" structure,
390 capable of binding iron. According to the "CELLO 2.5" software, Ape has a dominant
391 cytoplasmic localization (score of 2.418) but is also present at the outer membrane (1.652)
392 (Figure 2B). This canonical sub-cellular localization of a transmembrane protein is in
393 accordance with previous results finding this protein in the outer membrane proteome
394 (Moumene et al., 2015).

396 **rApe protein shows O-glycosylated post-traductional modifications**

397 Western blot analysis showed that rApe was detected with an anti-O-GlcNAc antibody at the
398 expected size of 66kDa (Figure 3). This size confirmed the data obtained by mass
399 spectrometry and is 30% larger than the one estimated by the amino acid sequence
400 encoded by *ape* gene (41 kDa for 365 amino acids). [The identity of rApe protein sequence](#)
401 [blasted with the possible major ferric iron binding protein precursor \(Q5FFA9\)](#). Altogether
402 these results demonstrate the O-glycosylation of rApe.

a supprimé:

404 **Enzymatic treatment of BAEC with chondroitinase decreases invasion by *E.*** 405 ***ruminantium***

a supprimé: ï

406 To investigate whether GAGs have a role in *E. ruminantium* adhesion process, BAEC were
407 treated with [chondroitinase](#) and then infected with *E. ruminantium*. The number of bacteria
408 was calculated at the end of growth, during the lysis of the BAEC, by qPCR Sol1 for each
409 treatment. After treatment with [chondroitinase](#) at 0.2U/mL, the FC corresponding to the
410 bacterial amount differential was higher than for the condition without treatment but this may

a supprimé: chondroitinase

a supprimé: chondroitinase

415 be explained by inter-well variability (Figure 4). Increasing [chondroitinase](#) concentrations to
416 0.4 and 0.9U/mL resulted in FC of 0.52 and 0.58, respectively, corresponding to a 50%
417 reduction of the number of bacteria compared to the untreated condition, highlighting the
418 role of [chondroitin](#) sulfate and dermatan sulfate in adhesion of *E. ruminantium* to the cell.
419 No affinity of rApe for heparan sulfate could be revealed using HRP anti-GFP antibody (data
420 not shown).

a supprimé: chondroitinase

421

422 **rApe binds to BAEC**

423 To go further in the understanding of the role of Ape in *E. ruminantium* invasion of host cells,
424 we analyzed the interaction of rApe with the surface of endothelial cells using flow cytometry.
425 Adhesion of recombinant proteins to BAEC was measured using flow cytometry to detect
426 the fluorescence of rApe harboring GFP tag. The dot plot profile clearly showed that the
427 percentage of labelled BAEC with rApe increases with the amount of rApe protein (Figure
428 5). As a negative control, the auto-fluorescence of the cells was measured on cells without
429 recombinant protein incubation. The percentage of labelled cells increased with protein
430 concentration up to 36 µg, showing a dose-effect relationship. Above these concentrations,
431 [bending of the curve starts](#) with 50% of rApe labelled BAE.

a supprimé: chondroitin

a supprimé: Ehrlichia

432

433 **Ape interacts with BAEC lysate, membrane and organelles cell fractions**

434 The Far Western blot shows the interaction between rApe and the cell fractions as well as
435 the lysate of the BAEC. rApe interacted with proteins of the cell lysate and more specifically
436 with those of the membrane and organelle fraction (Figure 6).

a supprimé: saturation occurred

437

438 **rApe coated beads adhere to BAEC and start internalization mechanism**

439 The visualization of interaction between rApe and the host cell was possible through usage
440 of beads adsorbed with rApe (mimicking *E. ruminantium*) and incubated with BAEC.
441 Adhesion was evaluated by scanning electron microscopy. The negative control showed
442 that non-coated beads did not adhere to the surface of the BAEC, that harbor their classical
443 fried egg shape (Figure 7A). In contrast, Figure 7B showed swollen BAEC, dotted with rApe
444 adsorbed beads after 30 minutes incubation, revealing an interaction between rApe and the
445 BAEC. Figure 7C displayed that rApe-coated beads also adhere (black arrow) and begin to
446 be invaginated (white arrow) by the endothelial cell membrane. Beads diameter did not
447 affect interaction of rApe and the BAEC. The images shown are representative of the
448 observations made in other fields. These data reinforcing the results obtained by

a supprimé: Ehrlichia

454 immunoblotting and flow cytometry prove that Ape interacts with the host cell membrane
455 and is involved in the adhesion of *E. ruminantium* to the host cell.

456

457 **Ape induces an antibody response in vaccinated goats**

458 In order to verify if *E. ruminantium* Ape protein induces a humoral response following
459 vaccination in goats, we tested sera from *in vivo* experiments on animals vaccinated with an
460 inactivated or attenuated bacterial vaccine (Marcelino et al. 2015 a, b). Goats #614 and #915
461 were both naïve prior to vaccination, characterized by the absence of antibodies against
462 Ape at 3 and 5 weeks post-vaccination, respectively (Figure 8). For #915, the ELISA test
463 showed an increase in humoral response against rApe over time. In fact, the antibody
464 response was developing between 5 and 7 weeks post-vaccination, the latter corresponding
465 to the vaccine boost. For goat #614, inoculation of an attenuated bacterial vaccine also
466 conduced to a humoral response, including response against rApe. These results suggest
467 that rApe could be a relevant target for further studies to see whether it could be a protective
468 immunogen in *E. ruminantium* infection *in vivo*.

469

470 **Discussion**

471 Controlled and determined *Ehrlichia* entry into host cell is a fundamental first step for an
472 effective infectious developmental cycle, particularly for an obligate intracellular pathogen
473 that strictly relies on its host to grow. In the last decade, comparative genomics and cellular
474 microbiology allowed major discoveries in the molecular pathogenesis of Anaplasmataceae.
475 These integrated approaches led to the effective identification of several bacterial virulence
476 determinants (e.g. effectors and regulators) and their diverse mechanisms of action
477 (Martinez et al., 2005; Cheng et al., 2008); (Rikihisa, 2017); Marcelino et al., 2015b ;
478 (Moumene et al., 2017). Notably, Rikihisa et al. identified that the EtpE protein governs the
479 binding and entry of *E. chaffeensis* into its host cells (Mohan Kumar et al., 2013). The binding
480 of EtpE to DNaseX elicits a signaling cascade that results in cytoskeleton modification,
481 filopodial induction and finally endocytosis into the host cell (Green et al., 2020). Previous
482 studies demonstrated that functional conservations of molecular pathogenicity determinants
483 can occur between of *E. chaffeensis* and *E. ruminantium* (Moumene et al., 2017) but such
484 bacterial ligand was still unknown in *E. ruminantium* at the beginning of this study. Among
485 other Rickettsiales, a receptor-mediated endocytosis was only reported for *Rickettsia conorii*
486 (Moumene et al., 2017) ; (Martinez et al., 2005).

a supprimé :

a mis en forme : Police :Non Italique

Code de champ modifié

a mis en forme : Police :Non Italique

488 Our aim being to determine some major pathogenicity determinants of *E. ruminantium*, we
489 chose to analyze ERGA_CDS_01230 (Ape, UniProt Q5FFA9), a putative iron-transporter
490 previously identified in the outer-membrane proteome of *E. ruminantium* (Moumene et al.,
491 2015). Indeed, we postulated that some key bacterial proteins involved in the early
492 interaction with the eukaryotic host cell should be overexpressed at early stages of the
493 developmental cycle and at the bacterial-host interface. Moreover, we previously showed
494 that iron was a triggering environmental cue for several *E. ruminantium* molecular virulence
495 determinants. Indeed, iron depletion induced a master regulatory gene, genes encoding
496 outer-membrane proteins of the Map1 family and genes of the Type IV Secretion System, a
497 major bacterial pathogenicity determinant (Moumene et al., 2017). Therefore, taking into
498 account that iron is a virulence triggering signal of *Ehrlichia*, Ape protein being a putative
499 iron transporter made it an excellent candidate for further characterization. In the present
500 study, we focused on the role of Ape protein in the interaction between *E. ruminantium* and
501 its mammalian host cell, notably during adhesion. As depicted in our working model for *E.*
502 *ruminantium* binding and invasion of its host endothelial cell (Figure 9), we showed that Ape
503 epitopes are recognized by the immune system of goats vaccinated with live attenuated
504 strain or killed strain or *E. ruminantium*. Indeed, after vaccination, we detected Ape
505 antibodies in sera of vaccinated goats indicating a global humoral response. Following this
506 model, the initial binding of *E. ruminantium* onto the host cell surface seems to involve
507 glycosaminoglycans (GAGs) as [chondroitinase](#) treatment of BAEC resulted in a significant
508 decrease of the number of bacteria present at the end of development cycle. The *ape* gene
509 is highly expressed at the elementary body developmental stages of *E. ruminantium*,
510 particularly during host cell lysis which precedes *E. ruminantium* release from host cells to
511 initiate a new cycle of infection. Interestingly, recombinant protein rApe is an O-glycosylated
512 protein that interacts with cell membrane and latex beads coated with rApe were able to
513 adhere to the BAEC surface to initiate internalization and follows a similar pattern of entry
514 like that of *E. ruminantium* (Moumene and Meyer, 2015).

515 Our results showed that Ape protein, an *Ehrlichia* ligand different from previously identified
516 *E. chaffeensis* EtpE (Mohan Kumar et al., 2013), is important for *E. ruminantium* adhesion
517 to the mammalian host cells. The mechanisms used by *E. ruminantium* to invade its host
518 are still not elucidated compared to other pathogens of the order *Rickettsiales*. Indeed
519 *Rickettsia conorii* uses OmpA (Hillman et al., 2013) to adhere to the host cell whereas two
520 different receptors were described for *Anaplasma marginale* and *A. phagocytophilum*
521 mobilizing Msp1a and OmpA (de la Fuente et al., 2003), (Hebert et al., 2017), Asp14 and

a supprimé: chondroitinase

a supprimé:

524 OmpA (Kahlon et al., 2013), (Ojogun et al., 2012), respectively to attach cell membrane.
525 Adhesins and invasins were largely described in other bacteria as surface located structures
526 for specific interaction with host cell receptors (Niemann et al., 2004). *Yersinia* outer
527 membrane invasin interacts with β 1 integrin receptors, inducing several reactions including
528 actin rearrangements at the site of bacterial entry, promoting invasion. *Salmonella*
529 translocates several effectors into target cells, some of them allowing the initial uptake of
530 the bacterium, whereas *Listeria* uses InIA and InIB-dependent molecular pathways, (Pizarro-
531 Cerda and Cossart, 2006). Ligands often show elongated molecules containing domains
532 commonly found in eukaryotic proteins (Niemann et al., 2004).

533 We showed that rApe is O-glycosylated. Post-translational modifications are one of the most
534 important mechanisms for activating, changing, or suppressing protein functions, being
535 widely used by pathogens to interact with their hosts. *E. ruminantium* glycoproteomics
536 showed a high percentage of glycoproteins, many of them being O-glycosylated (Marcelino
537 et al., 2019). *E. ruminantium* "mucin", which is also glycosylated, was presented as an
538 adhesin for tick cells, reinforcing a role of glycans in *Ehrlichia* adhesin molecules (de la
539 Fuente et al., 2004). The strength of ligand-receptor bacterial interactions is optimized
540 depending on their environment but weak enough to allow a bacterium to detach regularly
541 and migrate to other locations (Formosa-Dague et al., 2018). Glycan-glycan interactions in
542 bacterial-mammalian cells systems were characterized as low-affinity weak interactions
543 preceding high-affinity protein-glycan or protein-protein interactions but recent studies have
544 documented the importance of such interactions in bacterial adhesion (Formosa-Dague et
545 al., 2018). Indeed, we determined that the presence GAG on the surface of BAE plays a key
546 role in the attachment of *Ehrlichia* to bovine endothelial cells *in vitro*, reinforcing the
547 hypothesis that several receptors are probably required in *E. ruminantium* adhesion and
548 subsequent infection of host cells. [Chondroitinase](#) treatment significantly affected *Ehrlichia*
549 entry compared to the untreated condition. The enzymatic digestion of [chondroitin](#) and
550 dermatan from BAEC reduced the rate of infection of the BAEC, as *E. ruminantium* can no
551 longer adhere to the surface of the cells. Indeed, in other models like Chlamydia, GAGs
552 were shown to be used for initial attachment to host cells (Tiwari et al., 2012); Lyme disease
553 *Borreliae* requires glycosaminoglycan binding activity to colonize and disseminate to tissues
554 (Lin et al., 2017). Even though heparan sulfate appears to be the most important GAG
555 species involved in bacterial binding, both heparan sulfate and [chondroitin](#) sulfate were able
556 to influence the attachment of mucoid *P. aeruginosa*, *H. influenza* and *B. cepacia* in specific
557 ways that were dependent on the cell line involved (Martin et al., 2019). *Borrelia burgdorferi*

a supprimé: Chondroïtinase

a supprimé: chondroïtin

a supprimé:

a supprimé: chondroïtin

562 has multiple surface proteins with different binding specificities to GAGs depending on the
563 tissue affected (Leong et al., 1998). Different GAGs act as receptors for *B. burgdorferi*
564 depending on the host cells; both heparin sulfate and heparan sulfate are essential in
565 adherence to primary endothelium and adult kidney Vero cells, but only dermatan sulfate is
566 involved in attachment to human embryonic kidney cells (Garcia et al., 2016).

567 Although we did not establish the interaction of rApe adhesion with a cellular receptor, we
568 can still hypothesize that Ape actively triggers *Ehrlichia* internalization by the mean of a
569 ligand/receptor interaction. Kumar *et al.* already suggested the existence of additional
570 mammalian receptors for *Ehrlichia* infection (Mohan Kumar et al., 2013). The present study
571 identified the bacterial of a putative second *Ehrlichia* invasion-receptor pair and highlights
572 the importance of this molecular control of invasion for the *Anaplasmataceae* intracellular
573 bacteria. The probable existence of several ligand-receptor systems could indeed serve the
574 bacteria to infect a broader host range of animal reservoirs and vector ticks. Moreover, GAG
575 degradation following [chondroitinase](#) treatment severely impaired *Ehrlichia* infection. This
576 suggests that Ape could interact with a glycosylphosphatidylinositol (GPI)-anchored protein
577 as previously shown for PSGL-1 that is required for the binding and infection of human HL-
578 60 cells by *A. phagocytophylum* (Herron et al., 2000), This remains to be further studied as
579 well as its role in iron uptake of *Ehrlichia ruminantium* (Reneer et al., 2008).

580 In summary, with the identification of Ape (ERGA_CDS_01230), we found the first *Ehrlichia*
581 *ruminantium* protein that is involved in host cell invasion. Whether the *E. chaffeensis* EtpE
582 homolog (ERGA_CDS_08340) is functional in *E. ruminantium* remain to be explored, but
583 these outer-membrane proteins can now be considered as immune-dominant pathogen-
584 associated molecular patterns (Budachetri et al., 2020). Our next step is now [to](#) investigate
585 the use of rApe as a new vaccine candidate against Heartwater. In light of the lack of
586 prophylactic measures against *Ehrlichia* spp. and the rising appearance of antibiotic
587 resistances, deep understanding of invasion mechanisms is of prime importance and will
588 help to propose efficient alternative therapeutics blocking the early interaction between
589 these obligate intracellular bacteria and their host cells.

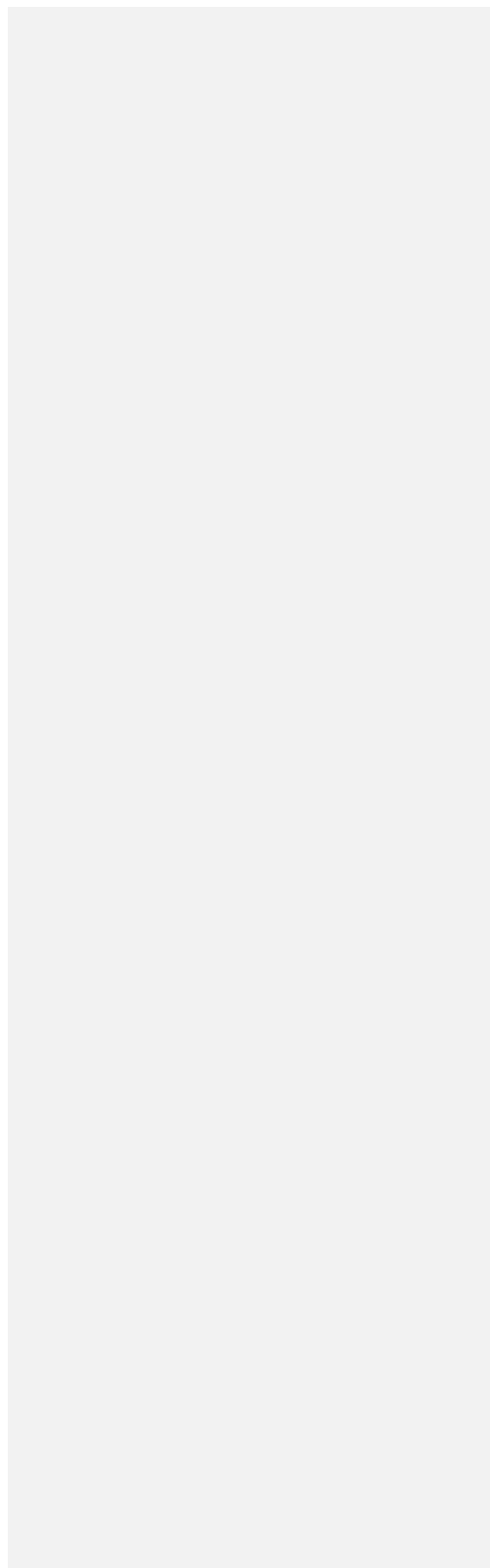
590

591 **Acknowledgements and funding information**

592 The authors acknowledge the financial support from Franco-Slovak bilateral project PHC
593 Stephanik 2014 n°31798XB and from European Union in the framework of the European
594 Regional Development Fund (ERDF), n° 2015-FED-186, MALIN project "Surveillance,
595 diagnosis, control and impact of infectious diseases of humans, animals and plants in

a supprimé: chondroitinase

597 tropical islands". We also gratefully acknowledge Géraldine Bossard and Valérie Rodrigues
598 for technical assistance in the development of ELISA assays.



599 **References**

- 600 Allsopp, B.A. (2010). Natural history of Ehrlichia ruminantium. *Vet Parasitol* 167, 123-135.
- 601 Aquino, R.S., Lee, E.S., and Park, P.W. (2010). Diverse functions of glycosaminoglycans in infectious diseases. *Prog Mol Biol Transl Sci* 93, 373-394.
- 602 Aquino, R.S., Teng, Y.H., and Park, P.W. (2018). Glycobiology of syndecan-1 in bacterial infections. *Biochem Soc Trans.*
- 603 Bartlett, A.H., and Park, P.W. (2010). Proteoglycans in host-pathogen interactions: molecular mechanisms and therapeutic implications. *Expert Rev Mol Med* 12, e5.
- 604 Bioscience, J. (2011). LEXSInduce 3 Expression Kit for inducible expression of recombinant proteins in *Leishmania tarentolae*. 28.
- 605 Brown, R.N., Romine, M.F., Schepmoes, A.A., Smith, R.D., and Lipton, M.S. (2010). Mapping the subcellular proteome of *Shewanella oneidensis* MR-1 using sarkosyl-based fractionation and LC-MS/MS protein identification. *J Proteome Res* 9, 4454-4463.
- 606 Budachetri, K., Teymournejad, O., Lin, M., Yan, Q., Mestres-Villanueva, M., Brock, G.N., and Rikihisa, Y. (2020). An Entry-Triggering Protein of Ehrlichia Is a New Vaccine Candidate against Tick-Borne Human Monocytic Ehrlichiosis. *mBio* 11.
- 607 Cangı, N., Gordon, J.L., Bournez, L., Pinarello, V., Aprelon, R., Huber, K., Lefrancois, T., Neves, L., Meyer, D.F., and Vachieri, N. (2016). Recombination Is a Major Driving Force of Genetic Diversity in the Anaplasmataceae Ehrlichia ruminantium. *Front Cell Infect Microbiol* 6, 111.
- 608 Cangı, N., Pinarello, V., Bournez, L., Lefrancois, T., Albina, E., Neves, L., and Vachieri, N. (2017). Efficient high-throughput molecular method to detect *Ehrlichia ruminantium* in ticks. *Parasit Vectors* 10, 566.
- 609 Cheng, Z., Wang, X., and Rikihisa, Y. (2008). Regulation of type IV secretion apparatus genes during Ehrlichia chaffeensis intracellular development by a previously unidentified protein. *J Bacteriol* 190, 2096-2105.
- 610 De La Fuente, J., Garcia-Garcia, J.C., Barbet, A.F., Blouin, E.F., and Kocan, K.M. (2004). Adhesion of outer membrane proteins containing tandem repeats of *Anaplasma* and *Ehrlichia* species (Rickettsiales: *Anaplasmataceae*) to tick cells. *Vet Microbiol* 98, 313-322.
- 611 De La Fuente, J., Garcia-Garcia, J.C., Blouin, E.F., and Kocan, K.M. (2003). Characterization of the functional domain of major surface protein 1a involved in adhesion of the rickettsia *Anaplasma marginale* to host cells. *Vet Microbiol* 91, 265-283.
- 612 Deem, S.L. (1998). A review of heartwater and the threat of introduction of *Cowdria ruminantium* and *Amblyomma* spp. ticks to the American mainland. *J Zoo Wildl Med* 29, 109-113.
- 613 Delano, W.L. (2009). The PyMOL molecular graphics system.
- 614 Dumler, J.S., Barbet, A.F., Bekker, C.P., Dasch, G.A., Palmer, G.H., Ray, S.C., Rikihisa, Y., and Rurangirwa, F.R. (2001). Reorganization of genera in the families *Rickettsiaceae* and *Anaplasmataceae* in the order Rickettsiales: unification of some species of *Ehrlichia* with *Anaplasma*, *Cowdria* with *Ehrlichia* and *Ehrlichia* with *Neorickettsia*, descriptions of six new species combinations and designation of Ehrlichia equi and 'HGE agent' as subjective synonyms of *Ehrlichia phagocytophila*. *Int J Syst Evol Microbiol* 51, 2145-2165.
- 615 Formosa-Dague, C., Castelain, M., Martin-Yken, H., Dunker, K., Dague, E., and Sletmoen, M. (2018). The Role of Glycans in Bacterial Adhesion to Mucosal Surfaces: How Can Single-Molecule Techniques Advance Our Understanding? *Microorganisms* 6.
- 616 Frutos, R., Viari, A., Ferraz, C., Bensaid, A., Morgat, A., Boyer, F., Coissac, E., Vachieri, N., Demaille, J., and Martinez, D. (2006). Comparative genomics of three strains of *Ehrlichia ruminantium*: a review. *Ann N Y Acad Sci* 1081, 417-433.
- 617 Frutos, R., Viari, A., Vachieri, N., Boyer, F., and Martinez, D. (2007). Ehrlichia ruminantium: genomic and evolutionary features. *Trends Parasitol* 23, 414-419.
- 618 Gagoski, D., Mureev, S., Giles, N., Johnston, W., Dahmer-Heath, M., Skalamera, D., Gonda, T.J., and Alexandrov, K. (2015). Gateway-compatible vectors for high-throughput protein expression in pro- and eukaryotic cell-free systems. *J Biotechnol* 195, 1-7.
- 619 Garcia, B., Merayo-Lloves, J., Martin, C., Alcalde, I., Quiros, L.M., and Vazquez, F. (2016). Surface Proteoglycans as Mediators in Bacterial Pathogens Infections. *Front Microbiol* 7, 220.
- 620 Green, R.S., Izac, J.R., Naimi, W.A., O'bier, N., Breitschwerdt, E.B., Marconi, R.T., and Carlyon, J.A. (2020). Ehrlichia chaffeensis EplA Interaction With Host Cell Protein Disulfide Isomerase Promotes Infection. *Front Cell Infect Microbiol* 10, 500.
- 621 Hebert, K.S., Seidman, D., Oki, A.T., Izac, J., Emani, S., Oliver, L.D., Jr., Miller, D.P., Tegels, B.K., Kannagi, R., Marconi, R.T., and Carlyon, J.A. (2017). Anaplasma marginale Outer Membrane Protein A Is an Adhesin That Recognizes Sialylated and Fucosylated Glycans and Functionally Depends on an Essential Binding Domain. *Infect Immun* 85.
- 622 Herron, M.J., Nelson, C.M., Larson, J., Snapp, K.R., Kansas, G.S., and Goodman, J.L. (2000). Intracellular parasitism by the human granulocytic ehrlichiosis bacterium through the P-selectin ligand, PSGL-1. *Science* 288, 1653-1656.

a mis en forme : Anglais (E.U)

a mis en forme : Anglais (E.U)

a mis en forme : Anglais (E.U)

658 Hillman, R.D., Baktash, Y.M., and Martinez, J.J. (2013). OmpA-mediated rickettsial adherence to and invasion of human
659 endothelial cells is dependent upon interaction with alpha2beta1 integrin. *Cell Microbiol* 15, 727-741.

660 Jonquieres, R., Pizarro-Cerda, J., and Cossart, P. (2001). Synergy between the N- and C-terminal domains of InlB for
661 efficient invasion of non-phagocytic cells by *Listeria monocytogenes*. *Mol Microbiol* 42, 955-965.

662 Kahlon, A., Ojogun, N., Ragland, S.A., Seidman, D., Troese, M.J., Ottens, A.K., Mastronunzio, J.E., Truchan, H.K.,
663 Walker, N.J., Borjesson, D.L., Fikrig, E., and Carlyon, J.A. (2013). *Anaplasma phagocytophilum* Asp14 is an
664 invasin that interacts with mammalian host cells via its C terminus to facilitate infection. *Infect Immun* 81, 65-
665 79.

666 Kobayashi, K., Kato, K., Sugi, T., Takemae, H., Pandey, K., Gong, H., Tohya, Y., and Akashi, H. (2010). *Plasmodium*
667 *falciparum* BAEBL binds to heparan sulfate proteoglycans on the human erythrocyte surface. *J Biol Chem* 285,
668 1716-1725.

669 Leong, J.M., Robbins, D., Rosenfeld, L., Lahiri, B., and Parveen, N. (1998). Structural requirements for
670 glycosaminoglycan recognition by the Lyme disease spirochete, *Borrelia burgdorferi*. *Infect Immun* 66, 6045-
671 6048.

672 Lin, M., Liu, H., Xiong, Q., Niu, H., Cheng, Z., Yamamoto, A., and Rikihisa, Y. (2016). Ehrlichia secretes Etf-1 to induce
673 autophagy and capture nutrients for its growth through RAB5 and class III phosphatidylinositol 3-kinase.
674 *Autophagy* 12, 2145-2166.

675 Lin, Y.P., Li, L., Zhang, F., and Linhardt, R.J. (2017). *Borrelia burgdorferi* glycosaminoglycan-binding proteins: a
676 potential target for new therapeutics against Lyme disease. *Microbiology* 163, 1759-1766.

677 Lundberg, M., Wikstrom, S., and Johansson, M. (2003). Cell surface adherence and endocytosis of protein transduction
678 domains. *Mol Ther* 8, 143-150.

679 Marcelino, I., Colome-Calls, N., Holzmuller, P., Lisacek, F., Reynaud, Y., Canals, F., and Vachiery, N. (2019). Sweet
680 and Sour Ehrlichia: Glycoproteomics and Phosphoproteomics Reveal New Players in Ehrlichia ruminantium
681 Physiology and Pathogenesis. *Front Microbiol* 10, 450.

682 Marcelino, I., Verissimo, C., Sousa, M.F., Carrondo, M.J., and Alves, P.M. (2005). Characterization of *Ehrlichia*
683 *ruminantium* replication and release kinetics in endothelial cell cultures. *Vet Microbiol* 110, 87-96.

684 Martin, C., Lozano-Iturbe, V., Giron, R.M., Vazquez-Espinosa, E., Rodriguez, D., Merayo-Lloves, J., Vazquez, F.,
685 Quiros, L.M., and Garcia, B. (2019). Glycosaminoglycans are differentially involved in bacterial binding to
686 healthy and cystic fibrosis lung cells. *J Cyst Fibros* 18, e19-e25.

687 Martinez, D., Coisne, S., Sheikboudou, C., and Jongejan, F. (1993). Detection of antibodies to *Cowdria ruminantium* in the
688 serum of domestic ruminants by indirect ELISA. *Rev Elev Med Vet Pays Trop* 46, 115-120.

689 Martinez, E., Cantet, F., Fava, L., Norville, I., and Bonazzi, M. (2014). Identification of OmpA, a *Coxiella burnetii* protein
690 involved in host cell invasion, by multi-phenotypic high-content screening. *PLoS Pathog* 10, e1004013.

691 Martinez, J.J., Seveau, S., Veiga, E., Matsuyama, S., and Cossart, P. (2005). Ku70, a component of DNA-dependent
692 protein kinase, is a mammalian receptor for Rickettsia conorii. *Cell* 123, 1013-1023.

693 Miller, E.M., and Nickoloff, J.A. (1995). *Escherichia coli* electrotransformation. *Methods Mol Biol* 47, 105-113.

694 Mohan Kumar, D., Yamaguchi, M., Miura, K., Lin, M., Los, M., Coy, J.F., and Rikihisa, Y. (2013). *Ehrlichia chaffeensis*
695 uses its surface protein EtpE to bind GPI-anchored protein DNase X and trigger entry into mammalian cells.
696 *PLoS Pathog* 9, e1003666.

697 Moumene, A., Gonzalez-Rizzo, S., Lefrancois, T., Vachiery, N., and Meyer, D.F. (2017). Iron Starvation Conditions
698 Upregulate *Ehrlichia ruminantium* Type IV Secretion System, tr1 Transcription Factor and map1 Genes Family
699 through the Master Regulatory Protein ErxR. *Front Cell Infect Microbiol* 7, 535.

700 Moumene, A., Marcelino, I., Ventosa, M., Gros, O., Lefrancois, T., Vachiery, N., Meyer, D.F., and Coelho, A.V. (2015).
701 Proteomic profiling of the outer membrane fraction of the obligate intracellular bacterial pathogen *Ehrlichia*
702 *ruminantium*. *PLoS One* 10, e0116758.

703 Moumene, A., and Meyer, D.F. (2015). *Ehrlichia's* molecular tricks to manipulate their host cells. *Microbes Infect.*

704 Niemann, H.H., Schubert, W.D., and Heinz, D.W. (2004). Adhesins and invasins of pathogenic bacteria: a structural view.
705 *Microbes Infect* 6, 101-112.

706 Noroy, C., Lefrancois, T., and Meyer, D.F. (2019). Searching algorithm for Type IV effector proteins (S4TE) 2.0:
707 Improved tools for Type IV effector prediction, analysis and comparison in proteobacteria. *PLoS Comput Biol*
708 15, e1006847.

709 Ojogun, N., Kahlon, A., Ragland, S.A., Troese, M.J., Mastronunzio, J.E., Walker, N.J., Viebrock, L., Thomas, R.J.,
710 Borjesson, D.L., Fikrig, E., and Carlyon, J.A. (2012). *Anaplasma phagocytophilum* outer membrane protein A
711 interacts with sialylated glycoproteins to promote infection of mammalian host cells. *Infect Immun* 80, 3748-
712 3760.

713 Perez, J.M., Martinez, D., Sheikboudou, C., Jongejan, F., and Bensaid, A. (1998). Characterization of variable
714 immunodominant antigens of *Cowdria ruminantium* by ELISA and immunoblots. *Parasite Immunol* 20, 613-
715 622.

716 Pizarro-Cerda, J., and Cossart, P. (2006). Bacterial adhesion and entry into host cells. *Cell* 124, 715-727.

717 Pruneau, L., Emboule, L., Gely, P., Marcelino, I., Mari, B., Pinarello, V., Sheikboudou, C., Martinez, D., Daigle, F.,

718 Lefrancois, T., Meyer, D.F., and Vachieri, N. (2012). Global gene expression profiling of *Ehrlichia ruminantium*
719 at different stages of development. *FEMS Immunol Med Microbiol* 64, 66-73.

720 Rajas, O., Quiros, L.M., Ortega, M., Vazquez-Espinosa, E., Merayo-Llodes, J., Vazquez, F., and Garcia, B. (2017).
721 Glycosaminoglycans are involved in bacterial adherence to lung cells. *BMC Infect Dis* 17, 319.

722 Reneer, D.V., Troese, M.J., Huang, B., Kearns, S.A., and Carlyon, J.A. (2008). Anaplasma phagocytophilum PSGL-1-
723 independent infection does not require Syk and leads to less efficient AnkA delivery. *Cell Microbiol* 10, 1827-
724 1838.

725 Rikihisa, Y. (2017). Role and Function of the Type IV Secretion System in Anaplasma and Ehrlichia Species. *Curr Top*
726 *Microbiol Immunol* 413, 297-321.

727 Sava, I.G., Zhang, F., Toma, I., Theilacker, C., Li, B., Baumert, T.F., Holst, O., Linhardt, R.J., and Huebner, J. (2009).
728 Novel interactions of glycosaminoglycans and bacterial glycolipids mediate binding of enterococci to human
729 cells. *J Biol Chem* 284, 18194-18201.

730 Teymournejad, O., Lin, M., and Rikihisa, Y. (2017). Ehrlichia chaffeensis and Its Invasin EtpE Block Reactive Oxygen
731 Species Generation by Macrophages in a DNase X-Dependent Manner. *mBio* 8.

732 Tiwari, V., Maus, E., Sigar, I.M., Ramsey, K.H., and Shukla, D. (2012). Role of heparan sulfate in sexually transmitted
733 infections. *Glycobiology* 22, 1402-1412.

734 Truttmann, M.C., Rhomberg, T.A., and Dehio, C. (2011). Combined action of the type IV secretion effector proteins
735 BepC and BepF promotes invasome formation of Bartonella henselae on endothelial and epithelial cells. *Cell*
736 *Microbiol* 13, 284-299.

737 Waterhouse, A., Bertoni, M., Bienert, S., Studer, G., Tauriello, G., Gumienny, R., Heer, F.T., De Beer, T.a.P., Rempfer,
738 C., Bordoli, L., Lepore, R., and Schwede, T. (2018). SWISS-MODEL: homology modelling of protein structures
739 and complexes. *Nucleic Acids Res* 46, W296-W303.

740 Xiaogen Zhou, W.Z., Yang Li, Robin Pearce, Chengxin Zhang, Eric W. Bell, Guijun Zhang, and Yang Zhang (2022). I-
741 TASSER-MTD: A deep-learning based platform for multi-domain protein structure and function prediction.
742 *Nature Protocols, in press*.

743 Yan, Q., Lin, M., Huang, W., Teymournejad, O., Johnson, J.M., Hays, F.A., Liang, Z., Li, G., and Rikihisa, Y. (2018).
744 Ehrlichia type IV secretion system effector Etf-2 binds to active RAB5 and delays endosome maturation. *Proc*
745 *Natl Acad Sci U S A* 115, E8977-E8986.

746 Yang, J., and Zhang, Y. (2015). I-TASSER server: new development for protein structure and function predictions.
747 *Nucleic Acids Res* 43, W174-181.

748 Yu, C.S., Chen, Y.C., Lu, C.H., and Hwang, J.K. (2006). Prediction of protein subcellular localization. *Proteins* 64, 643-
749 651.

750

751 **Figure captions**

752 **Figure 1. Temporal expression of the (ERGA_CDS_01230) *ape* gene in *E. ruminantium***
753 **determined by qRTPCR.**

754 (A) *E. ruminantium* sigmoidal growth curve was determined by qPCR targeting *pCS20*
755 region and represented as [relative bacterial number](#) along the cycle of development

a supprimé: log 10

756 (B) Transcript levels were determined from 24, 48, 72 and 120 hpi by qRTPCR targeting
757 ERGA_CDS_01230 gene. Levels were normalized by the quantity of bacteria measured by
758 qPCR Sol1 and the ratio was compared to 96 hpi, allowing fold-change (FC) determination,
759 expressed as log 2. Values at each time point are the means +/- standard deviations for 2
760 biological replicates. Gp38 is for *E. ruminantium* Gardel strain, passage #38 (virulent strain).

761

762 **Figure 2. Structural characterization of Ape protein.**

763 (A-H) I-TASSER-MTD derived [3D](#)-prediction of the ERGA_CDS_01230 gene product ([Ape](#)
764 [protein in green](#)) interacting with [oxo-iron molecule](#) (red). Front (A-B), back (C-D) and side
765 (E-F) views of Ape showing [a succession of \$\alpha\$ -helices \(turquoise\)](#) linked by loops ([pink](#))
766 distributed around [\$\beta\$ -sheets \(purple\)](#), organized as a three-dimensional "c-clamp" structure.
767 [The enlarged panels \(G-H\) of the binding site allow the visualization of the residues involved](#)
768 [in polar \(yellow\) and non polar \(light blue\) interactions. The oxo-iron molecule \(CIN1\)](#)
769 [constituted by 3 atoms of iron \(orange\) and 12 atoms of oxygen \(red\) interacts with Ape](#)
770 [protein \(green\) via polar interaction \(hydrogen bond with T99 in yellow\) and non-polar](#)
771 [interactions \(hydrophobic interactions in light blue involving L120 and Q122\) bonds.](#)

a supprimé: s

a supprimé:

a supprimé: a

a supprimé:

a supprimé:

772 (J) Reliability score prediction by CELLO 2.5 software of the subcellular localization of the
773 native *E. ruminantium* Ape protein. Ape presents a typical subcellular localization of an
774 active transporter, with a dominant cytoplasmic localization and is also present at the outer
775 membrane.

a supprimé: B

776

a supprimé: ¶

777 **Figure 3. rApe is an O-glycosylated recombinant protein.**

778 Composite picture of a Western blot detecting O-glycosylation of recombinant Ape protein
779 (lane 2). Recombinant proteins were separated by SDS-PAGE, then transferred to PVDF
780 and incubated with anti-O-GlcNAc antibody. The Western blot was probed with anti-mouse
781 IgM-HRP antibody and revealed by TMB substrate. Lane 1: negative control : [BSA](#); lane 2:
782 rApe. Numbers and black arrowheads indicate molecular masses in kilodaltons (kDa). The
783 recognized rApe is significantly larger (66 kDa) than the one predicted by the amino acid
784 sequences encoded by ERGA_CDS_01230 gene (41 kDa).

793

794 **Figure 4. Chondroitinase impairs BAEC infection by *E. ruminantium*.** Using 0.4 and
795 0.9U/mL [chondroitinase](#) resulted in a halving of the number of bacteria compared to the
796 untreated condition. Bacterial quantification was performed at lysis stage by qPCR sol1 after
797 [chondroitinase](#) treatment at three different concentration. Fold-change (FC) was obtained
798 by calculating the bacterial amount differential for each condition compared to the condition
799 without treatment and represented as $2^{-\Delta\Delta Ct}$.

800

801 **Figure 5. rApe attaches to the host cells.**

802 Different concentrations of rApe tagged with GFP were incubated with BAEC. Adherence of
803 GFP-rApe to prefixed BAEC was evaluated by flow cytometry and showed a dose-effect
804 relationship up to 36 μ g of rApe. Fluorescent-labelled cells quantified by flow cytometry are
805 represented in % for each concentration point. Auto-fluorescence was evaluated with cells
806 without recombinant protein.

807

808 **Figure 6. rApe interacts with cell lysate and membrane fractions.**

809 Composite picture of a Far-Western blot detecting Ape protein. Lysate and cell fractions
810 were separated by SDS-PAGE, transferred to PVDF and incubated either with rApe (left
811 panel) or PBS as a negative control (right panel). The Western blot was probed with rabbit
812 anti-GFP-HRP antibody, and revealed by peroxide substrate mixed with chromogen DAB.
813 1: protein ladder, 2 and 5: cell lysate, 3: cytoskeleton fraction, 4 and 6: membrane and
814 organelles fraction.

815

816 **Figure 7. rApe is sufficient for adhesion of latex beads to bovine endothelial cells.**

817 Representative images of BAEC incubated 30 minutes with fluorescent latex beads
818 (1.82×10^8) coated with rApe and processed for scanning electron microscopy.

819 (A) Endothelial cells did not retain non-adsorbed beads (0.1 μ m diameter) on their cell
820 surface. (B) On the opposite, the whole surface of the same type of cells are covered with
821 adherent beads (0.5 μ m diameter) absorbed with rApe. (C) Enlarged view of adherent beads.
822 Such beads present two kinds of localizations. Some of them are already internalized (black
823 arrow heads) while others are still located outside the cell remaining in contact with the
824 cytoplasmic membrane (white arrow heads). Scale bars are indicated.

825

826 **Figure 8. Ape induces an antibody response in sera of vaccinated goats.**

a supprimé: Chondroitinase

a supprimé: chondroitinase

a supprimé: chondroitinase

830 The antibody response to Ape during vaccination kinetic was tested by ELISA. Sera of
831 vaccinated goats were incubated in wells coated with rApe, followed by incubation with anti-
832 goat antibody coupled to HRP. Antibody response was detected by ELISA titers (optical
833 density at 450 nm). Shown are representative results from five vaccinated goats. #614: goat
834 vaccinated with an attenuated vaccine. #915: goat vaccinated with an inactivated vaccine.
835 The time (in weeks) post-vaccination is indicated. Goats vaccinated with inactivated vaccine
836 were also challenged for resistance to *E. ruminantium* Gardel strain seven weeks post
837 vaccination.

838

839 **Figure 9. Schematic representation of *Ehrlichia ruminantium* binding to mammalian
840 cells and rApe interaction with the host cell surface.**

841 Ape is located at *E. ruminantium* outer membrane and is recognized by antibody from sera
842 of vaccinated animals. *E. ruminantium* can adhere and enter into BAEC but infection is
843 reduced when GAG like [chondroitin](#) and dermatan sulfate are degraded. The recombinant
844 version of *E. ruminantium*, rApe, is glycosylated and latex beads coated with rApe bind to
845 BAE cell surface and start to enter in BAEC, in a similar manner that of *E. ruminantium*.
846 Whether Ape binds to a cellular receptor and the following triggered signaling cascade
847 remain to be determined.

a supprimé: chondroïtine

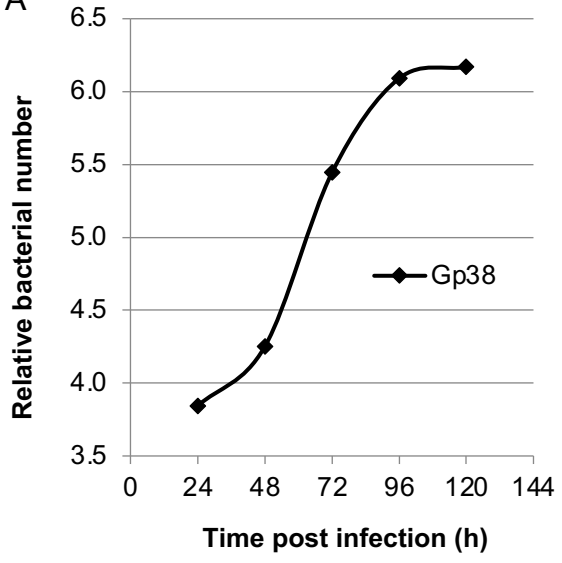
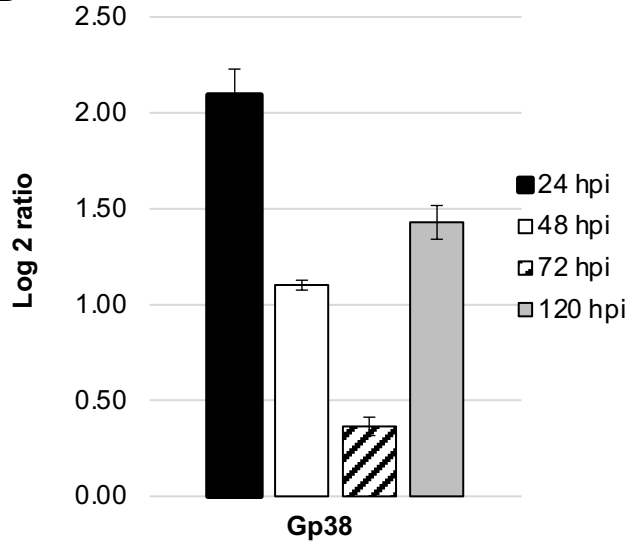
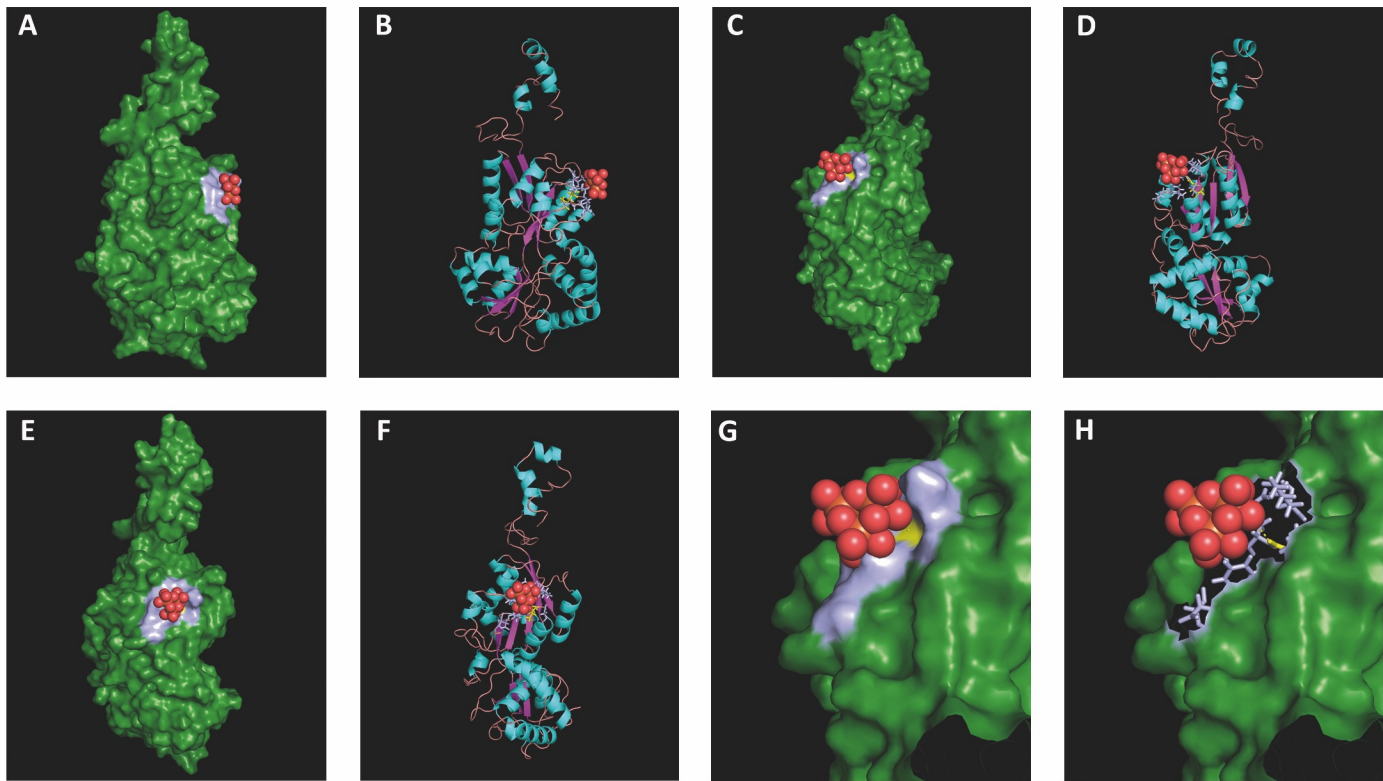
A**B**

Figure 1



I

BACTERIAL LOCALIZATION	ERGA_CDS_01230
Cytoplasmic	2,418
Outer membrane	1,652
Periplasmic	0,424
Inner membrane	0,404
Extracellular	0,102

Figure 2

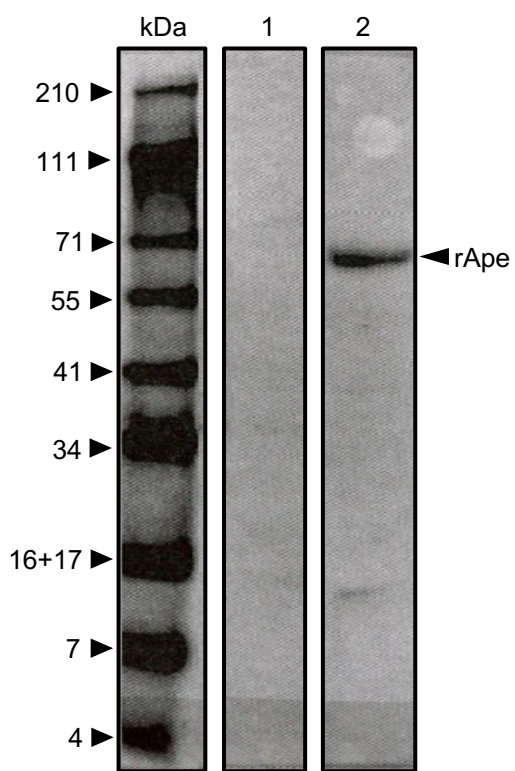


Figure 3

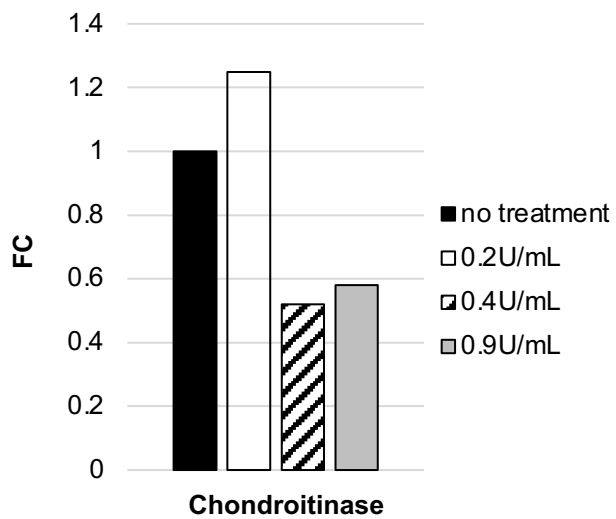


Figure 4

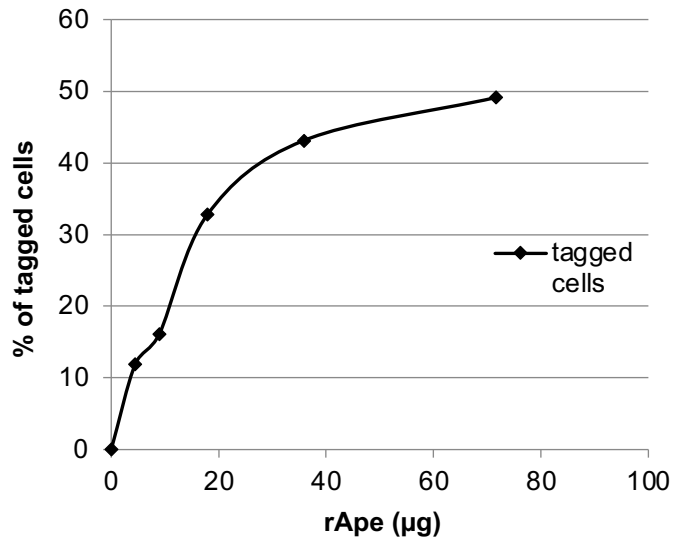


Figure 5

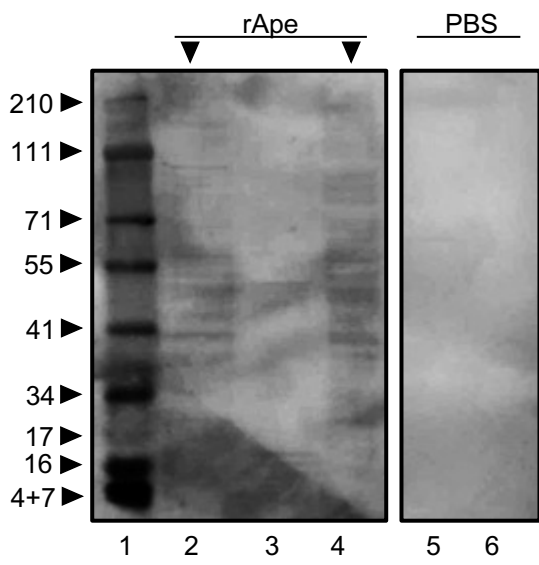


Figure 6

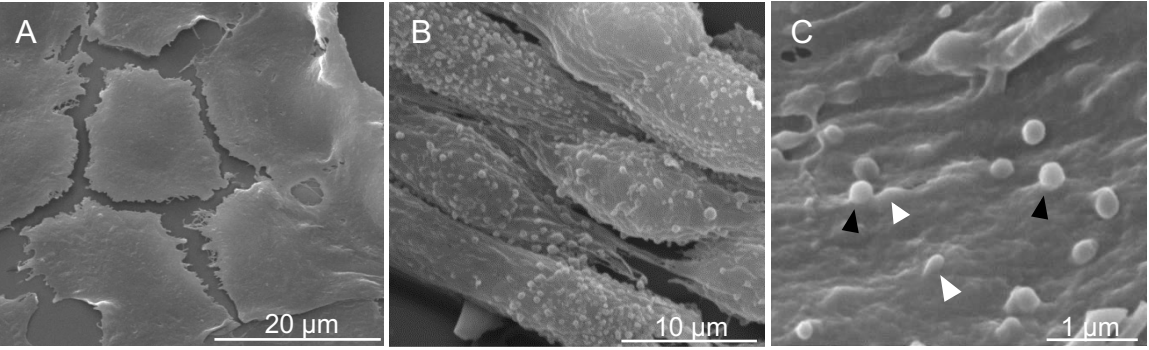


Figure 7

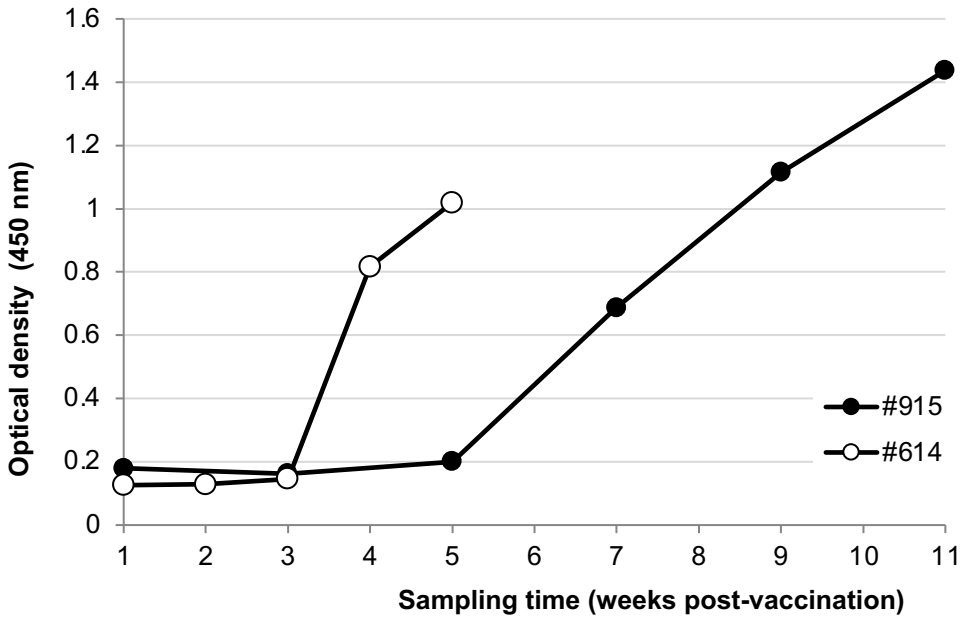


Figure 8

